Polymer Testing 117 (2023) 107849

Contents lists available at ScienceDirect

Polymer Testing

journal homepage: www.elsevier.com/locate/polytest

Development of a new birthing model material based on silicone rubber/ natural rubber blend

Phanutchanart Panmanee [a], Manunya Okhawilai [a,b], Phattarin Mora [c], Chanchira Jubsilp [c], Panagiotis Karagiannidis [d], Sarawut Rimdusit [a,*]

[a] Research Unit in Polymeric Materials for Medical Practice Devices, Department of Chemical Engineering, Faculty of Engineering, Chulalongkorn University, Bangkok, 10330, Thailand
[b] Metallurgy and Materials Science Research Institute, Chulalongkorn University, Bangkok, 10330, Thailand
[c] Department of Chemical Engineering, Faculty of Engineering, Srinakharinwirot University, Nakhonnayok, 26120, Thailand
[d] School of Engineering, Faculty of Technology, University of Sunderland, Sunderland, SR6 0DD, United Kingdom

ARTICLE INFO

Keywords:
Silicone rubber
Natural rubber
Sulfur/peroxide curing system

ABSTRACT

A novel material based on silicone rubber (SR) modified with natural rubber (NR) was developed. Combinations of sulfur/peroxide curing systems were used as crosslinking agents. The results showed that the incorporation of NR improved the tensile strength, tear strength and elongation at break of the SR/NR blend. It was also found that the blending of SR/NR at 90/10 provided the greatest tensile strength and elongation at break of 1.9 MPa and 1381%, respectively as well as good tear strength. The properties of this SR/NR blend and the corresponding interpenetrating polymer network (IPN) were compared and showed that the IPN provided higher tensile strength. However, the blend exhibited greater elongation at break and hardness, relatively close to human skin which are more important for a birthing model material. It can be concluded that the blending of SR/NR at 90/10 is the most promising material to substitute expensive currently used birthing model.

1. Introduction

Birthinganatomical models related to pregnancy and birth, are in great demand and commonly used by doctors and gynecologists for medical education. Birthing practice using simulating medical materials greatly enhance the experience of giving birth in the real situation. For a birthing model, it is noted that the material must be strong, tough, with very high elongation without tearing during stretching simulating vagina. Moreover, it must be able to recover to its original shape.

Silicone rubber (SR) has special features due to the unique molecular structure derived from the Si–O bond, and it possesses many advantages that other materials cannot replace. SR is superior to regular organic rubbers, in terms of heat resistance, chemical inertness, low surface tension, excellent electrical insulation, abrasion resistance, effective water repellency under high humidity conditions, weather ability resistance, and oxidation resistance [1,2]. It also has extremely low-temperature flexibility [3]. SR has developed for various simulating medical devices for example breast model for breast cancer screening [4], suture pad for medical practicing [5], drug released materials [6] and implantation [7]. Methyl vinyl silicone rubber (MVQ) is widely used in applications for example light emitting diode [8], stretchable electrodes and sensors [9,10], friction materials [11,12], and electromagnetic shielding [13–15]. T.T. Dang et al. observed that vinyl group in SR help increased mechanical properties in terms of tensile strength and modulus at 100% elongation and thermal properties compared to the SR without vinyl group [16]. It was related to that the presence of double bonds in vinyl group acted as active sites which further reacted with curing agent and underwent crosslink. In addition, when the vinyl group content increases, the crosslinking density also increases [17]. Chemical inertness, low toxicity and biocompatibility are most benefit properties for medical applications (surgical or pharmaceutical) [18]. However, poor mechanical properties of SR limit its application especially for birthing model. To overcome these problems, SRs are frequently blended or copolymerized with other polymers or rubbers. The tensile strength and elastic modulus of SR/LLDPE blend was increased by linear low -density polyethylene (LLDPE). The values were improved 2.5 and 3.5 times higher than that of the neat SR [19].

Natural rubber (NR) is one of the most effective rubbers for modifying the mechanical properties of SR, due to its technical and economic advantages, as well as a variety of useful properties, such as high

* Corresponding author.
E-mail address: Sarawut.r@chula.ac.th (S. Rimdusit).

https://doi.org/10.1016/j.polymertesting.2022.107849
Received 16 August 2022; Received in revised form 1 October 2022; Accepted 22 October 2022
Available online 30 October 2022

Table 1
Formulation of SR/NR blends and IPNs.

Composition (phr)	SR/NR compound ratios					
	100/0	95/5	90/10	85/15	80/20	70/30
SR	100	95	90	85	80	70
NR	0	5	10	15	20	30
Zinc oxide	2.5	2.5	2.5	2.5	2.5	2.5
Stearic acid	1	1	1	1	1	1
TMTD	0.05	0.05	0.05	0.05	0.05	0.05
TBBS	0.5	0.5	0.5	0.5	0.5	0.5
Sulfur	1	1	1	1	1	1
Peroxide	1	1	1	1	1	1

strength, high elasticity, high tearing resistance, abrasion resistance and dynamic mechanical properties. However, it has high tackiness, low thermal stability, and poor weather resilience, all of which could be improved by crosslinking its chain structure [16]. A system of SR having vinyl groups/NR/silica was reported to have improved tensile strength and elongation at break by 71% and 100%, respectively, compared to a system of SR without vinyl groups/NR/silica. The maximum elongation at break of 1200% was reached in the SR having vinyl groups/NR/silica [16]. There are many methods to crosslink polymer chains, depending on the characteristics of rubber and applications. The most popular methods are sulfur vulcanization or peroxide reaction. However, the use of sulfur has the disadvantage that it can cure rubber having double bonds in the molecule. Although using peroxide as a curing agent could solve the blooming of curing agent on the sample's surface, but it is expensive and difficult to control the reaction during rubber molecules crosslinking [17,20]. The mixing of sulfur and peroxide curing agents brought benefit to the rubber system as tensile strength of the SR having vinyl group/NR was enhanced to 44% and 29% of the samples cured with pure sulfur and pure peroxide, respectively [16]. However, the modulus at 100% elongation at break of the samples cured with combination of sulfur and peroxide decrease due to too low crosslink density. J'an Krůzel'ak et al. reported the use of mix curing agents in NR, styrene-butadiene rubber, acrylonitrile-butadiene rubber for rubber magnetic application [21]. The results showed that composition of curing agent has considerable effect on crosslink density of the system thus resulting in change of physical-mechanical properties. With increasing peroxide content, tensile strength was improved. Even intensive research on using mix curing agents of sulfur and peroxide, based on our knowledge, limit study of SR/NR system has been reported in which the type of polymer matrix is strongly influence overall properties of materials.

In this work, mechanical properties of SR are improved by blending with NR and cured with sulfur/peroxide combination for using as birthing model's materials. The effects of NR content on the mechanical properties, morphology and thermal properties of developed SR/NR blends are investigated in this work.

2. Experimental

2.1. Materials

SR (0.5–0.7 mmol/g of vinyl group) was purchased from HRS Co., Ltd. (Korea). NR (STR5L grade) was supplied by Tongthai rubber Co., Ltd. (Thailand). Sulfenamide accelerator including N-tert-butyl-2-benzothiazolylsulfenamide (TBBS) and thiuram accelerator including tetramethylthiuram disulfide (TMTD) were supplied by Kij Paiboon Chemical Co., Ltd. (Thailand). TBBS is a primary accelerator used to increase the speed of vulcanization and permit vulcanization to proceed at lower temperature and with greater efficiency. TMTD is a secondary accelerator used to activate the primary accelerator. Zinc oxide (ZnO) and stearic acid were purchased from Ajax Finechem Pty Ltd. (New Zealand) and AF Goodrich chemical Co., Ltd. (Thailand), respectively. Sulfur and 2,5-dimethyl-2,5-di(tert-butylperoxy)hexane were used as curing (crosslinking) system and supplied by Polymer Asia Co., Ltd. (Thailand).

2.2. Preparation of the SR/NR blends

NR was added in an internal mixer (model MX105-D40L50, Chareon Tut Co., LTd, Thailand) at a temperature of 80 °C and 80 rpm of rotor speed. SR, and accelerators were then added stepwise. After that sulfur/peroxide curing agent was added to generate the pre-cure characteristics. The mixing temperature was maintained at 80 °C throughout, and the total mixing time was 60 min. The SR/NR blends were cut in sheets of 2 mm thickness. These were used to make cured sheets by hot pressing at a temperature of 170 °C, pressure of 110 MPa for 15 min using compression molding machine. The formulation for SR/NR blends is shown in Table 1.

2.3. Preparation of the SR/NR IPN

Firstly, SR, accelerators, and sulfur/peroxide curing agent are added and mixed in an internal mixer at a temperature of 80 °C for 40 min. After that, the temperature was raised to 170 °C and the mixing procedure was processed for 15 min to fully vulcanize SR. Then, NR was mixed with SR at a temperature of 80 °C for 20 min. The compound was then transferred to compression molder and vulcanize at a temperature of 170 °C, pressure of 110 MPa for 15 min. The formulation for SR/NR IPN is also shown in Table 1.

2.4. Characterization

The chemical characteristics and network formation of the SR/NR blends were analyzed by using a Spectrum GX FT-IR spectrometer with an ATR accessory from PerkinElmer (Waltham, MA, USA). All spectra were scanned in the 4000–650 cm^{-1} wavenumber range. The curing behavior of the SR/NR blends were investigated using a differential scanning calorimeter (DSC) model DSC1 module from Mettler-Toledo (Thailand) Ltd. (Bangkok, Thailand). Each sample was sealed in an aluminum pan with a mass of about 5–10 mg. The temperature range was from 25 to 250 °C with a heating rate of 10 °C min^{-1} and a nitrogen flow rate of 50 mL min^{-1}. The tensile strength, modulus and elongation at break of the SR/NR blends were measured according to the ASTM D412 test method at room temperature by using dumbbell-shaped specimens punched out from molded rubber sheets by using a type C die. The tensile tests were carried out with a universal testing machine (UTM) model 5567 from Instron Co. Ltd. (Bangkok, Thailand), at a constant crosshead speed of 500 mm/min. The tear strength of the SR/NR blends was tested according to the ASTM D624 test method using a UTM model 5567 from Instron Co. Ltd. (Bangkok, Thailand). The tear test was conducted at the same temperature and crosshead speed as the tensile test. The tear strength was computed by using the following equation.

$$Tear\ Strength = \frac{Max\ Load\ (N)}{Thickness\ (mm)} \quad (1)$$

For the tension set analysis, the dumbbell-shaped specimens were stretched to 700% elongation (max elongation of the birthing model during childbirth) without being broken and were held at the specified elongation for 10 min at a room temperature. After removing the force, the specimen was allowed to rest for 10 min. The gauge length was measured before and after the test. The tension set was calculated by following equation (2).

$$Tension\ set\ (\%) = \frac{(L - L_0)}{L_0} \times 100 \quad (2)$$

where L = length after force removal for 10 min (mm)

L_0 = initial length (mm)

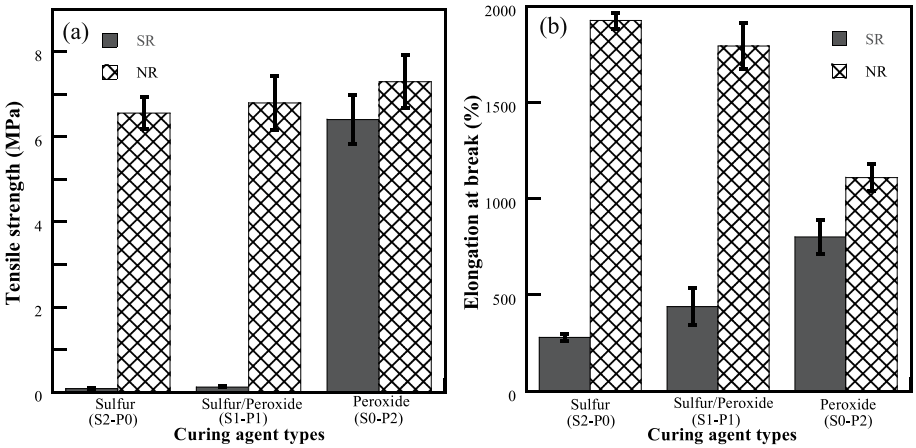

Fig. 1. Mechanical properties of SR and NR vulcanizates with different curing agents: (a) tensile strength and (b) elongation at break.

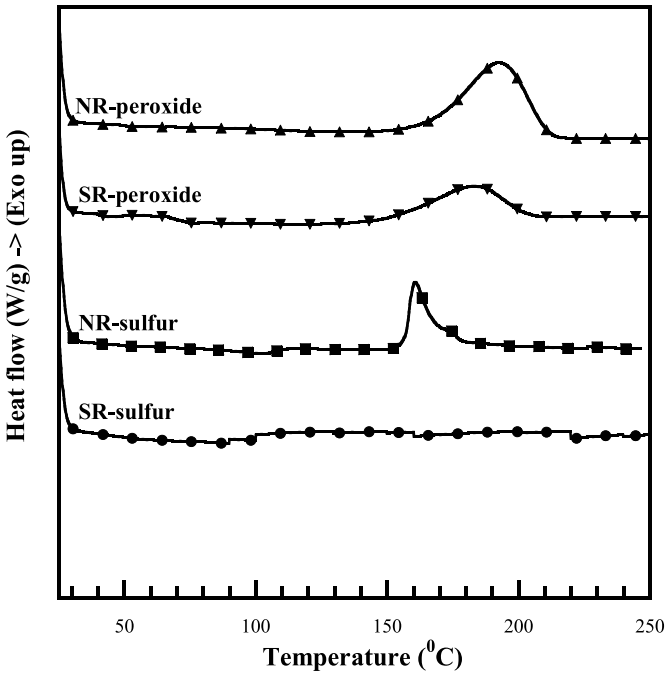

Fig. 2. DSC thermograms of the neat SR and NR cured with sulfur and peroxide.

The hardness of samples was tested with shore A durometer according to ASTM D2240. The crosslink density of the SR/NR blends was determined at equilibrium swelling state. The weight of SR/NR samples (W_1) was measured before immersion in toluene in a sealed vessel for 24 h. Then the swollen SR/NR samples were weighed (W_2). Subsequently, the samples were dried for 24 h in a vacuum oven at a temperature of 70 °C to remove all the solvent and get dried weight (W_3). The swelling ratio (Q), molecular weight between crosslinks (M_c), crosslink density (CLD), and gel fraction (g) were calculated according to Flory-Rehner equation as follows:

$$Q = \frac{(W_2 - W_1)/\rho_s}{W_1/\rho_r} \tag{3}$$

$$M_c = \frac{-\rho_r V_1 \left(\varphi_r^{\frac{1}{3}} - \frac{\varphi_r}{2}\right)}{Ln(1-\varphi_r) + \varphi_r + \chi_{12}\varphi_r^2} \text{where; } \varphi_r = \frac{1}{1+Q} \tag{4}$$

$$CLD = \frac{\rho_r N}{M_c} \tag{5}$$

$$g = \frac{W_3}{W_1} \tag{6}$$

where ρ_s and ρ_r are the densities of solvent (0.87 g/cm^3 for toluene) and rubber, respectively. φ_r is the volume fraction of polymer in the swollen sample. V_1 is the molar volume of the toluene solvent (106.54 ml/mol) where χ_{12} is the polymer–solvent interaction parameter (the values of χ_{12} are 0.465 for toluene) and N is Avogadro's number (6.02214179 × 10^{23}). Morphology and fracture surface of the SR/NR blends was investigated by a scanning electron microscope (SEM, model SU-4800, Hitachi) (Tokyo Japan) using an acceleration voltage of 5 kV. All specimens were coated with a thin coating layer of gold using a JEOL ion sputtering device (model JFC-1200). The glass transition temperature (T_g) of the SR/NR blends was determined using a dynamic mechanical analyzer (DMA1, Mettler Toledo, Switzerland) under single cantilever clamp mode. The SR/NR samples were cut into a rectangular bar with dimensions 5 mm × 30 mm × 2 mm. The testing was performed at a temperature range of −150 to 100 °C, with a heating rate of 3 °C min^{-1} and a frequency of 1 Hz.

3. Results and discussion

3.1. Mechanical and thermal properties of SR and NR vulcanizates

The values of mechanical properties of SR and NR vulcanizates prepared using different curing agents i.e. sulfur or peroxide or sulfur/peroxide system at a total concentration 2phr (mass parts per hundred parts of rubber) are illustrated in Fig. 1. The relatively low tensile strength of SR cured with sulfur was attributed to that the SR cannot be cured with sulfur, as was shown and by DSC (Fig. 2). The SR did not show a sulfur-cured peak revealing no vulcanization effect on the SR leading to a poor mechanical strength compared to NR. A similar behavior was also reported by Dang et al. (2010) as they did not observe a torque increment during curing process of SR with sulfur. Moreover, it was clearly proved that the tensile strength of SR and NR vulcanizates were improved with increasing the peroxide content as exhibited in Fig. 1. This is because peroxides were able to crosslink the SR or NR chains to create a three-dimensional network resulting in higher tensile strength values with increasing peroxide content. However, it was noticed that the tensile strength of SR slightly increased with peroxide content from 0 to 1 phr with the presence of sulfur. This is due to the hindering effect of sulfur atoms during the crosslinking of SR with peroxide leading to the unvulcanized network of SR [16]. The highest tensile strength of both SR and NR vulcanizates were observed to be 6.4

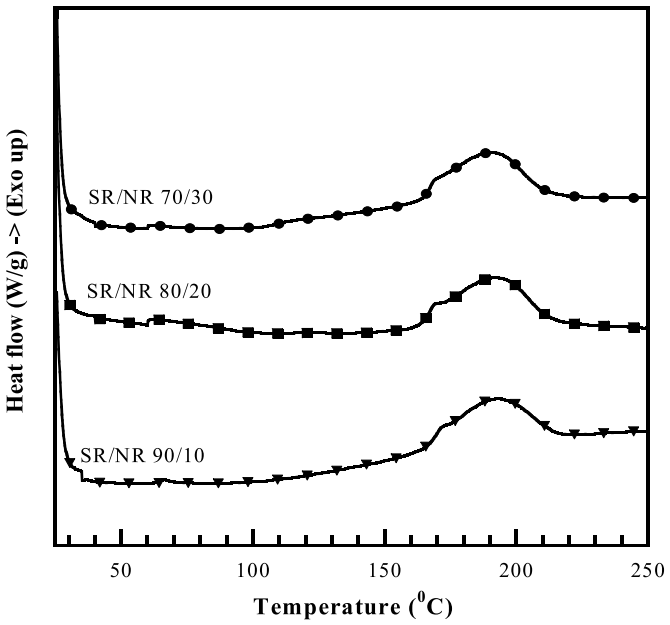

Fig. 3. DSC thermograms of the SR/NR blends with different NR content.

Table 2
Total heat of reaction ΔH_R, Tp_1 and Tp_2 at different NR content.

SR/NR mass ratios	ΔH_R (J/g)	T_{p1} (°C)	T_{p2} (°C)	$\Delta H_{R,p1}$ (J/g)	$\Delta H_{R,p2}$ (J/g)
90/10	10.42	175	193	1.17	9.24
80/20	10.77	172	191	1.15	9.62
70/30	11.25	171	191	1.08	10.17

and 7.3 MPa, respectively in the systems cured with neat peroxide (S0–P2). The results revealed that peroxide curing agent formed a higher crosslink network through C–C bonds with SR and NR. Furthermore, the results showed that not only the composition of curing system, but also the type of rubber matrix plays an important role to mechanical properties [22].

The effects of curing system on elongation at break values are shown in Fig. 1(b). The elongation at break of SR vulcanizates increased with the increasing peroxide content and reached a maximum elongation at break value at 808% for the sample cured with neat peroxide (S0–P2). On the other hand, SR which cannot be cured with sulfur exhibited a lower elongation at break. For the NR vulcanizates, the elongation at break increased with increasing the amount of sulfur having the highest elongation at break at 1925% for sample cured with neat sulfur (S2–P0). This is because the peroxide curing agent led to the formation of more rigid C–C bonds between rubber chain segments, resulting in restriction of the rubber chain mobility. Whereas, the more elastic sulfidic linkages were created during the crosslinking of sulfur with NR supporting the higher chain movement [22]. As a result, the elongation at the break of NR cured with sulfur was higher compared to that obtained by the peroxide curing system. Even the NR vulcanizate provided an elongation at break comparable or higher than that of commercial birthing model having the value of 1726%, the human-like texture of NR is far from being compared with SR. Furthermore, the SR vulcanizate exhibited less elongation at break than that requirement. Consequently, the SR/NR blends cured with the combination of sulfur/peroxide at 1:1 (S1–P1) were further studied. In comparison, the elongation at break of VQM significantly reduced after irradiation indicating the effect of chemical curing agents of peroxide and sulfur [23].

Fig. 2 demonstrates the DSC thermograms with the curing exothermic peaks of SR and NR with sulfur or peroxide curing agents. It can be seen that no vulcanization effect was observed on the neat SR heated with sulfur. In addition, the curing temperature was observed to be at 160 °C for the NR curing with sulfur and at 182–193 °C for SR and NR curing with peroxide suggesting that sulfur curing reaction occurred at a lower temperature compared to peroxide curing reaction.

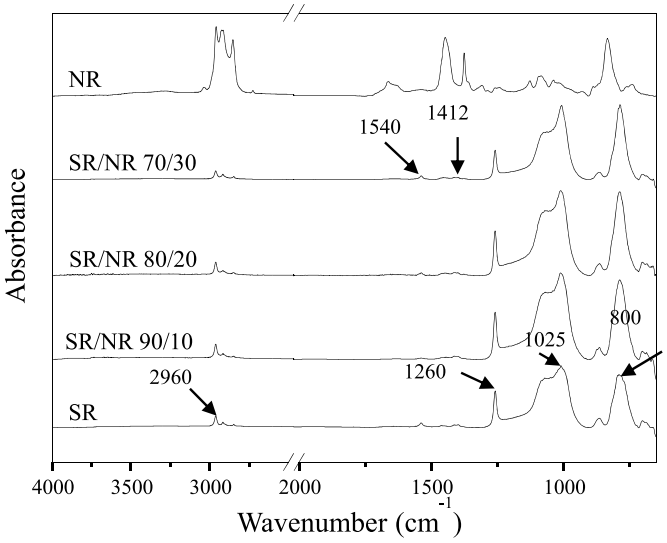

Fig. 5. FT-IR spectra of SR/NR blends having different SR/NR mass ratio.

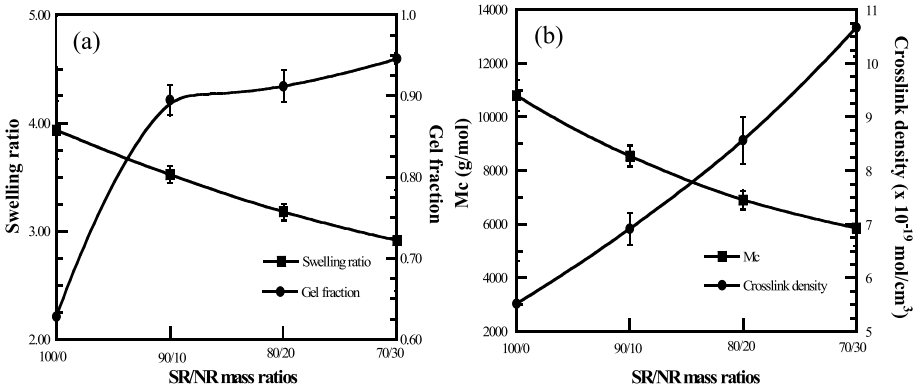

Fig. 4. (a) ( ) Swelling ratio and (●) gel fraction; (b) ( ) molecular weight between crosslinking and (●) Crosslink density of SR/NR blends having different SR/NR mass ratios.

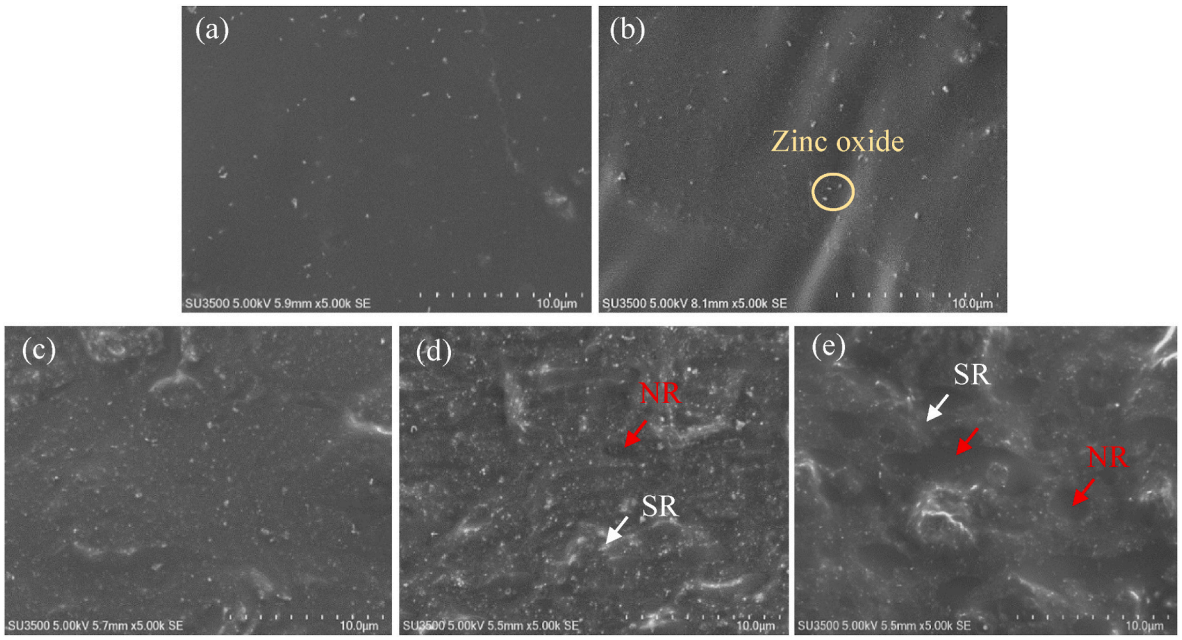

Fig. 6. SEM micrographs of (a) SR, (b) NR, SR/NR blends with NR contents at (c) 10 wt%, (d) 20 wt% and (e) 30 wt%.

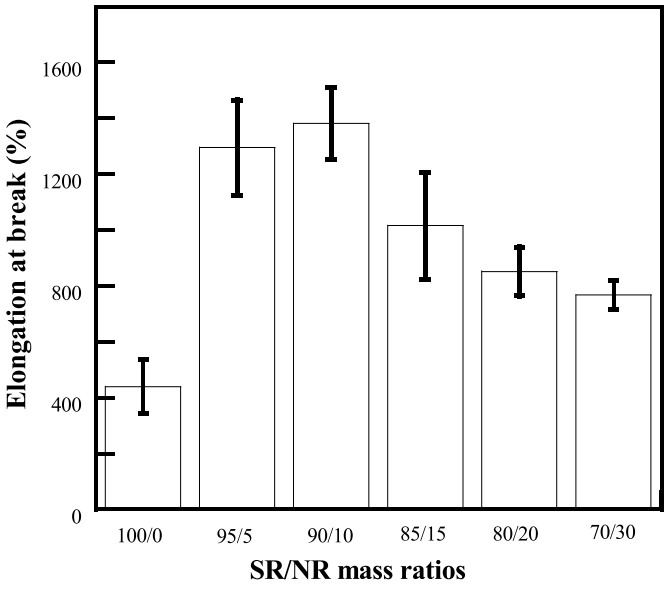

Fig. 7. Elongation at break of SR/NR blends having different SR/NR mass ratios.

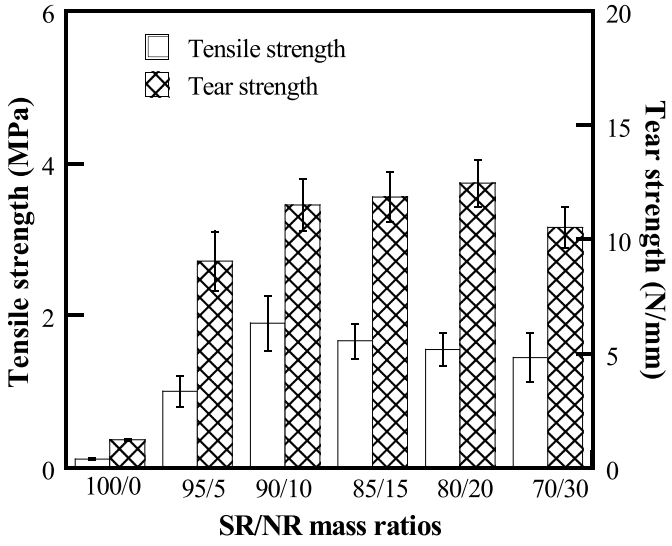

Fig. 8. Tensile strength and tear strength value of SR/NR blends with.

3.2. Curing behavior of SR/NR blends

The Effects of NR content on curing behavior of the SR/NR blends were studied by DSC (Fig. 3). The thermographs show the appearance of two exothermic overlapped peaks i.e. the first curing peak at 171–175 °C corresponding to the curing by sulfur and the later second peak at 191–193 °C to curing by peroxide. Table 2 summarizes the exothermic peak temperatures Tp_1, Tp_2 which correspond to curing by sulfur or peroxide respectively and (ΔH_R) corresponding to the heat of curing reaction.

It was observed that the curing peak temperature of SR/NR blends by the sulfur/peroxide system shifted to lower temperatures with increasing the NR content. It was because NR contains allylic group in its structure which readily react with the sulfur in sulfur curing system.

The dynamic heat obtained under the area of the curing peak temperature represents the total reaction heat of curing. Table 1 shows that with increasing NR content, the area under the sulfur curing peak decreased, while the area under the peroxide curing peak increased. This is because the addition of NR in the blend systems cause chemical decomposition of the peroxide initiator [24]. This is because NR has a π-bonded that can dissociate into radicals in the NR phase, which further reacted with peroxide curing agent and then produce a denser crosslinked network. In addition, it can be seen that the SR/NR blend with a mass ratio of 90/10 exhibited the highest ΔH_R,p_1, compared to the others indicating the highest crosslinking reaction between NR phase and sulfur. This trend was more obvious as the amount of NR in the system increased, the degree of sulfur crosslinking was decreased. On the other hand, as the amount of NR in the system increased i.e. for SR/NR blend with a ratio 70/30 higher heat of reaction was observed revealing higher degree of crosslinking with peroxide curing agent and these interactions reduced the molecular mobility of the matrix.

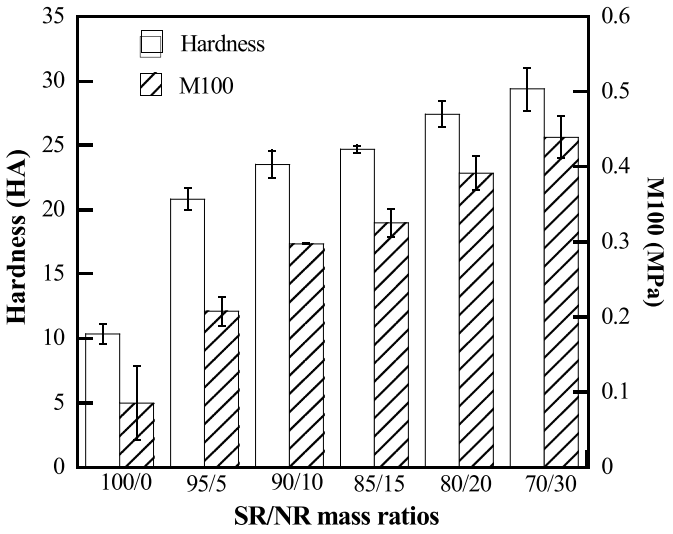

Fig. 9. Hardness and modulus at 100% elongation (M100) of SR/NR blends having different SR/NR mass ratios.

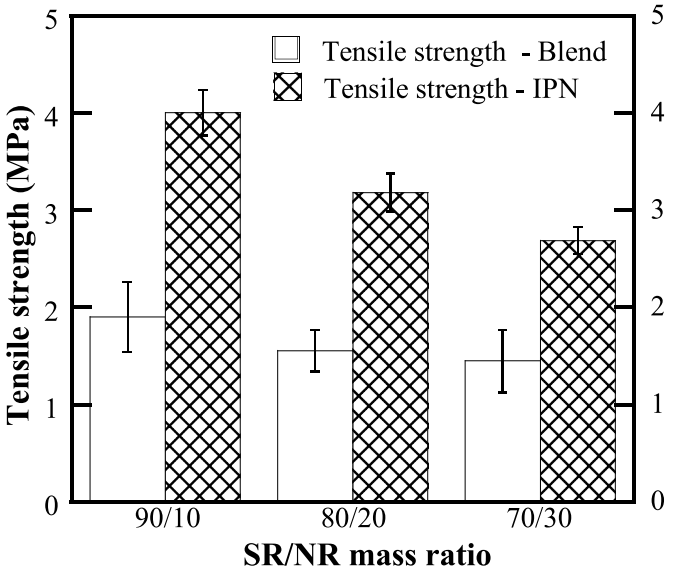

Fig. 10. Tensile strength value of SR/NR IPN and blends with different SR/NR mass ratios.

3.3. Swelling behavior of SR/NR blends

The swelling behavior of a polymeric network is a parameter that indicates the ability of solvent penetration into the void space between the polymeric chains network [25]. According to Hansen's solubility parameter theory, high polymer-solvent compatibility results from a similar solubility parameter between the polymer and the solvent; this permits the diffusion of the solvent into the polymer, leading to swelling and changes in the physical and chemical properties of the polymer. The performance of polymer applications suffers as a result of this tendency [26]. The parameters of swelling behavior consist of swelling ratio (Q), molecular weight between crosslinks (Mc), crosslink density (CLD), and gel fraction (g) which can be calculated based on Eqs (3)–(6), respectively. The effects of NR content on swelling behavior of SR/NR blends in toluene solvent are shown in Fig. 4(a). The swelling ratio of all SR/NR blends was lower than that of neat SR, and the swelling ratio of all SR/NR blends decreased with increasing NR content. Meanwhile, the gel fraction of all SR/NR blends which refers to the proportion of insoluble

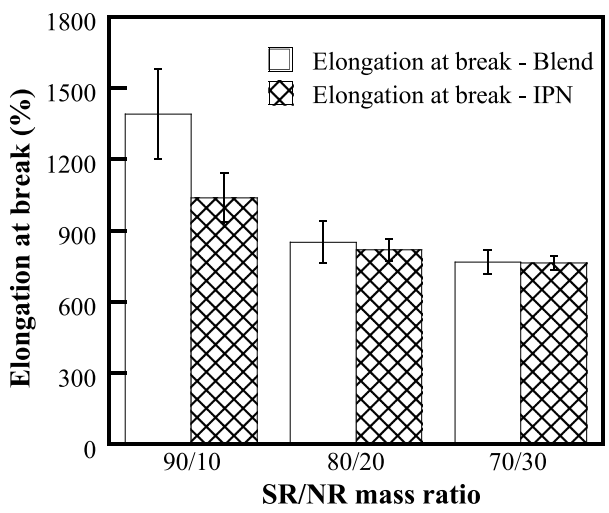

Fig. 11. Elongation at break of SR/NR IPN and blends having different SR/NR mass ratio.

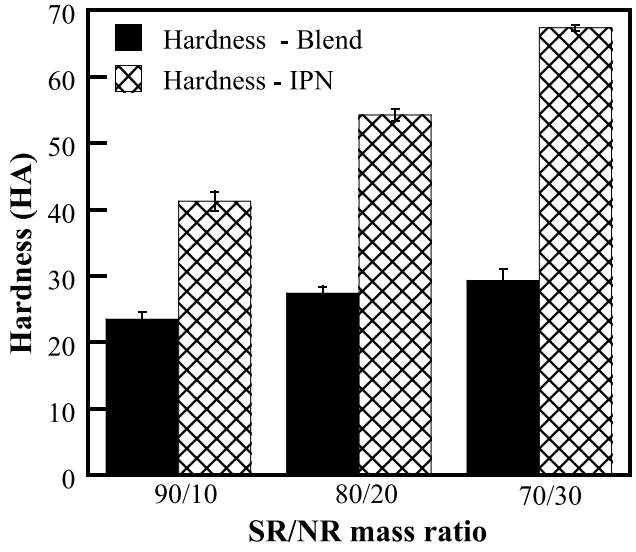

Fig. 12. Hardness value of SR/NR IPN and blends having different SR/NR mass ratio.

rubber weight to the initial weight of rubber were substantially higher than that of neat SR and slightly increased regarding the NR content. It was attributed to the presence of sulfur and peroxide as an initiator as cross-linker during the vulcanization process, which generate active sites on the NR chain, bonding together to form a crosslinked network, limiting the diffusion of solvent, resulting in a lower swelling ratio and higher gel content [26].

Fig. 4(b) shows that the values of molecular weight between the crosslinks decreased with higher NR content corresponding to higher crosslink density. It can be inferred that adding NR to SR/NR blends the solvent resistance of the blends improved.

3.4. Chemical structures of SR/NR blends

FT-IR spectra of SR/NR blends having different SR/NR mass ratios are presented in Fig. 5. The neat SR showed characteristic absorption bands at 1015 and 1087 cm^{-1} which are attributed to the stretching vibration of Si–O–Si on the backbone of SR. The sharp band at 800, 1260 and 2960 cm^{-1} were assigned to the scissoring vibration, bending vibration of Si–CH_3 and the stretching vibration of CH_3, respectively. The

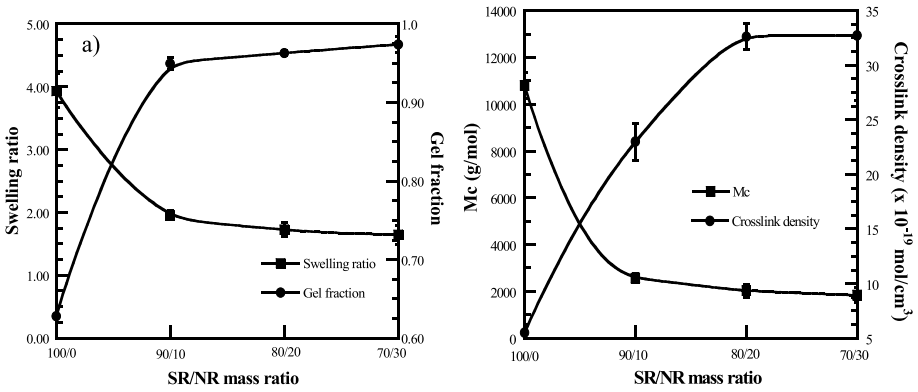

Fig. 13. (a) ( ) Swelling ratio and (•) gel fraction; (b) ( ) molecular weight between crosslinking and (•) Crosslink density of SR/NR IPNs having different SR/NR mass ratio.

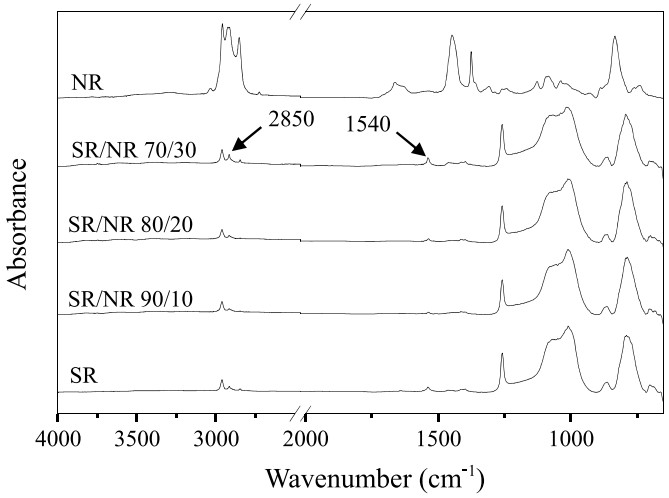

Fig. 14. FT-IR spectra of SR/NR IPN having different SR/NR mass ratio.

peak at 1412 cm^{-1} corresponds to the characteristic peak of the vinyl group.

The band at 1540 cm^{-1} is also observed which is related to zinc stearate, formed from the reaction between ZnO and stearic acid. It is noted that this characteristic peak showed a high intensity in SR/NR blends with higher NR content implying lower crosslinking density of the sulfur-cured system. This result agrees with the cure characteristics shown in Fig. 3. In addition, the lower peak intensity at 1412 cm^{-1} with lower SR contents was attributed to the consumption of double bonds of vinyl groups during the peroxide-vulcanized process. Vinyl groups was reported to be more reactive to form free radicals reacting with the crosslinking agent than the methyl groups [27]. Furthermore, it can be seen from the FT-IR spectra that no new peak or peak shifts were observed for the SR/NR blends with an addition of NR. This reveals the physical bonding between constituents of SR/NR blends.

3.5. Morphology of SR/NR blends

The fracture surface morphology of the neat SR, NR and SR/NR blends were observed by SEM. It can be seen from Fig. 6 that the fracture surface of the crosslinked SR and NR showed a uniform morphology, as also reported by Q. Wang et al. [28]. In contrast, the SR/NR blends exhibited a heterogeneous morphology similar to as observed by T.T. Nga Dang [19] which was due to different solubility parameter i.e. 7.3–7.5 $J^{1/2}/cm^{3/2}$ of SR [29] and 16.9 $J^{1/2}/cm^{3/2}$ of NR [30]. However, the boundary of the two domains of the SR/NR blend with 10 wt% of NR was less distinguishable, indicating partially miscible blend of those NR and SR networks. With higher NR content up to 30 wt%, an obvious phase separation was noticed causing poor interfacial interaction between the phases and resulting in the reduction of mechanical properties (tensile strength, elongation at break and tear strength) as previously discussed in the mechanical property analysis.

3.6. Mechanical properties of SR/NR blends

The elongation at break of a material is one of the most important properties for a birthing model. The elongation at break is correlated with the crosslink density of a polymer [22]. The effects of NR content on the elongation at break of the SR/NR blends having different SR/NR ratio at a fixed sulfur/peroxide curing system ratio of 1:1 are shown in Fig. 7. The elongation at break value of the neat SR was found to be 439%. An incorporation of NR into the SR/NR blends showed an improvement in elongation at break value. It is clearly apparent that the elongation at break of the SR/NR blends increased with increasing the amount of NR and reached the maximum value of 1381% at a mass ratio of 90/10. However, at higher NR content than 10 wt%, the elongation at break decreased. This is related to phase separation and the presence of double bonds in the NR chain causing higher degree of crosslink density [16]. NR has more double bonds in its structural units than SR, which could react well with sulfur and peroxide leading restriction of the polymer chains' mobility and consequently to the reduction of elongation at break. The elongation at break of materials of this research was higher than that developed in the system of polyoxymethylene/VQM/thermoplastic polyurethane ternary vulcanizate [31].

The tensile strength is an important value to determine the strength of the material. In Fig. 8, the tensile strength value of the neat SR was observed at 0.12 MPa. With an incorporation of NR in the range of 5 to 30 wt%, the values increased with increasing NR content and reach the maximum value of 1.9 MPa at the mass ratio of 90/10. This was due to NR crystallization under the stress (stress-induced crystallization) which helps the improvement of the inter-molecular attraction resulting in the reinforcement of the rubber [22]. Furthermore, the NR contained double bonds, a π–π negatively charged electron structure which attracted and reacted with sulfur and peroxide. The effects of the peroxide vulcanization on the tensile strength were apparently observed in the SR/NR blend systems with NR content more than 10 wt%. The tensile strength values slightly decreased with increasing NR content. This might be due to a more rigid crosslinked network formed with higher NR content, with restricted the mobility and orientation of elastomer chain segments [32]. In addition, the tensile strength of the SR/NR blends was higher than that of the birthing model's material having the value of 0.61 MPa so it is more preferable to use this SR/NR blend as a substitute of commercial birthing model's material.

The tear strength of the sample is one of the most essential

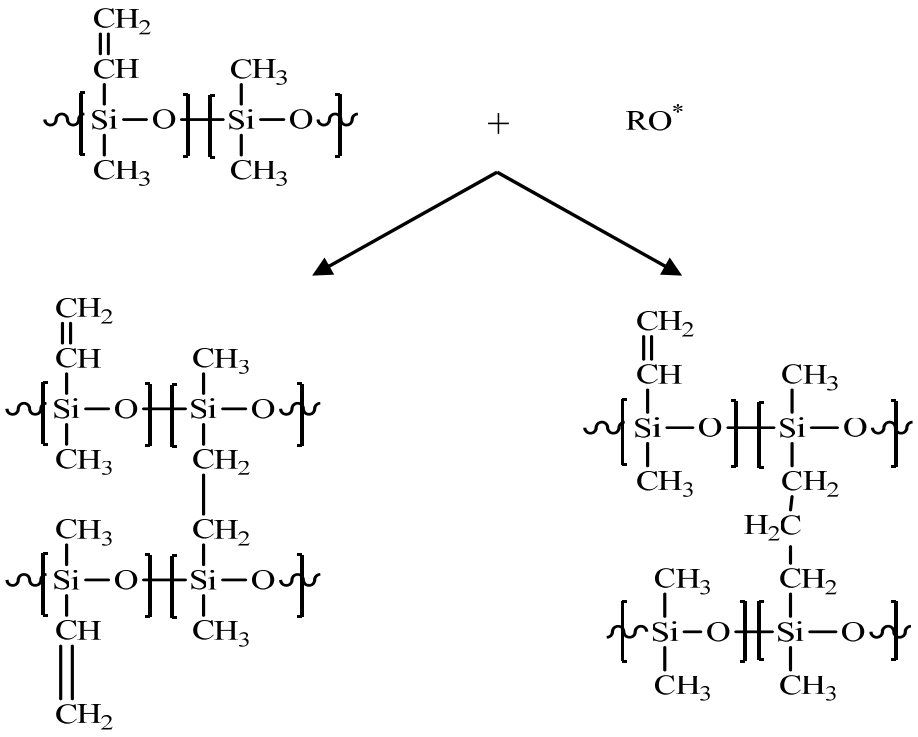

Fig. 15. Schematic of the possible structure of crosslinked SR with peroxide.

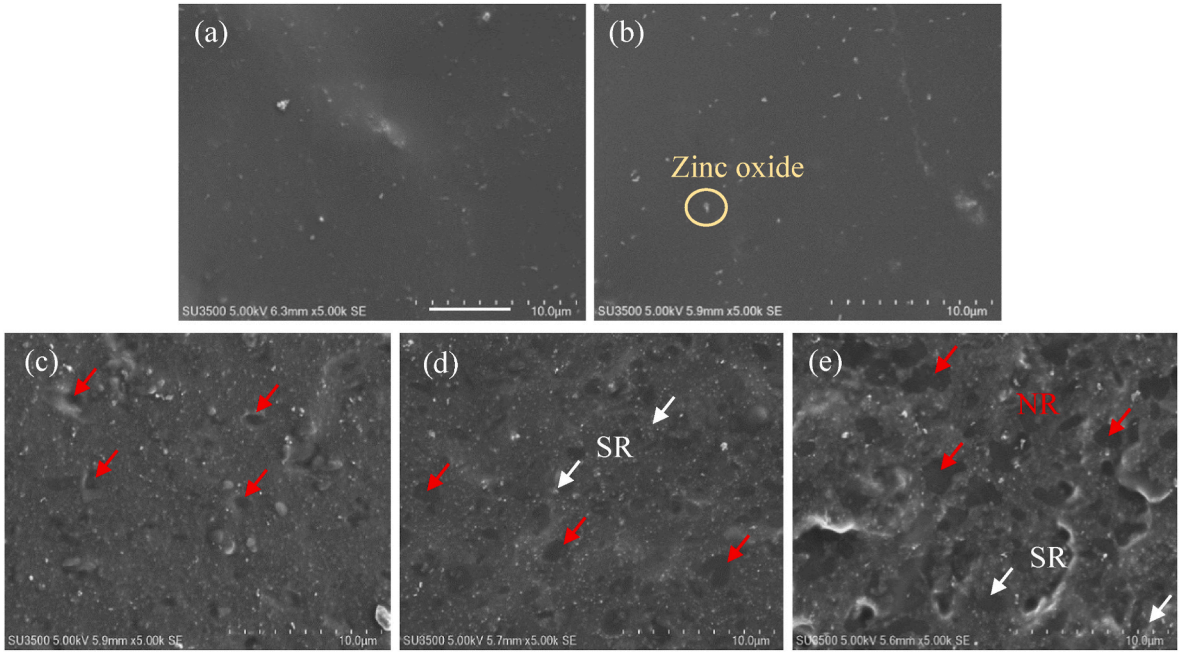

Fig. 16. SEM micrographs of (a) SR, (b) NR, SR/NR IPN with NR contents at (c) 10 wt%, (d) 20 wt% and (e) 30 wt%.

mechanical parameters characterization of birthing model's materials. It is the value of force required to rip a material and to make the crack continue until it fails. Fig. 8 shows the tear strength of the SR/NR blends with different NR content. With 5 to 20 wt% of NR in the blends, the tear strength of SR/NR improved significantly. A continuity of cross-linking network during the vulcanization was formed by the active sites of NR thus providing an increase of phase adhesion and obstruction of crack propagation [33]. In addition, higher crosslinking density was obtained with a higher amount of NR, resulting in an increase in tear strength. This behavior was also reported by Kuriakosa and De [34]. However, at higher NR content than 20 wt%, it is obviously seen that the agglomerated NR also prevented molecular chains movement of the blends.

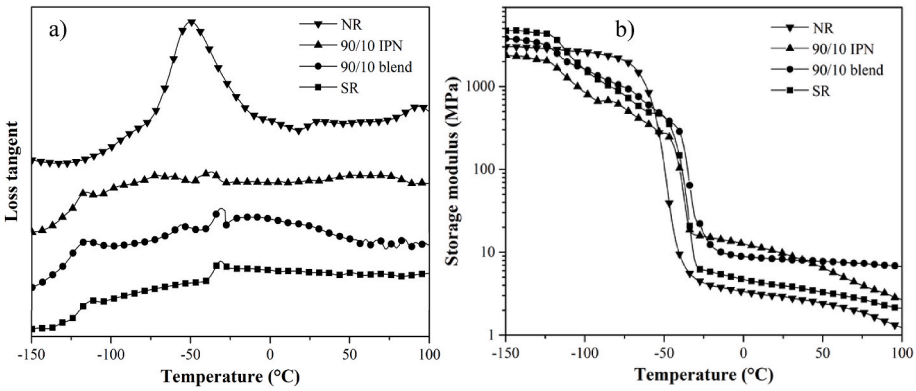

Fig. 17. (a) Loss tangent and (b) Storage modulus of SR/NR polymer hybrids; (■) neat SR, (●) SR/NR 90/10 blend, (▲) SR/NR 90/10 IPN, and (▼) neat NR.

Table 3
Dynamic mechanical properties of SR/NR polymer hybrids.

Sample	T_g (°C)		Storage Modulus at −150 °C (GPa)
	SR	NR	
SR	−110	–	4.68
SR/NR 90/10 blend	−118	−56	3.77
SR/NR 90/10 IPN	−117	−72	2.37
NR	–	−50	3.03

Table 4
Tension set of SR/NR polymer hybrid.

Sample	Tension set (%)
Birthing model's sample	11.3 ± 2.5
SR/NR 90/10 blend	12.8 ± 1.5
SR/NR 90/10 IPN	4.6 ± 1.8

This makes the movement of molecular chains to be more difficult contributing to weak points of the blends resulting in decreased tear strength [35].

different SR/NR mass ratios.

The effects of NR content on hardness and the tensile modulus at 100% elongation (M100) of the SR/NR blends are shown in Fig. 9. The hardness and M100 of the SR/NR blends are related to their cross-linking density [32]. From Fig. 6, it is clearly evident that the hardness of the neat SR was improved by incorporation of NR and the values increased linearly with NR content. This is because NR possess π-bonded functional groups that can dissociate with radicals in the NR phase which can react well with both sulfur and peroxide curing agents and cause a denser crosslinked network with less mobility of the rubber chain or higher stiffness. In addition, the M100 of the SR/NR blends also increased with increasing NR content in a similar tendency to hardness values [36] which corresponds to a higher cross-linking density.

3.7. Mechanical properties of SR/NR IPN

To gain some knowledge about the mechanical properties of SR/NR IPN we modify the network structure using mechanically labile bonding of the chains [37]. The effect of NR content on tensile strength of the blends and IPNs are shown in Fig. 10. It was obviously seen that the tensile strength of the SR/NR IPNs were higher than those of the blend systems. It was attributed to the greater chain entanglement between the SR and NR networks, which was a characteristic of IPNs [38]. Moreover, it can also be noticed that the tensile strength of SR/NR IPNs decreased with lower SR content due to a higher crosslinked density in the SR phase, resulting in higher stiffness and lower tensile strength.

Fig. 11 shows the effect of NR content in the SR/NR IPNs and blends on the elongation at break. At the same amount of NR, a substantial reduction in elongation at break was observed for the IPN compared to the blends resulting from an increase of network integrity. network. The IPN crosslinked structure caused a reduction in the rubber chain mobility, thus leading to a drastic reduction of elongation at break [38].

The hardness of the SR/NR blends and IPNs are illustrated in Fig. 12. It can be observed that the hardness values of the SR/NR IPNs increased, as the amount of SR decreased, which is due to the higher crosslinking density in the SR phase, leading to more rigid C–C bonds compared with the SR/NR blends at the same amount of SR. Moreover, the hardness values of the SR/NR IPNs were higher than those of the blends, indicating the more efficient crosslinked network formation of the IPNs than the blends [39]. Furthermore, the results showed that the hardness values of the SR/NP IPNs were higher than the average hardness value of human skin, which was reported to be about 20–30 HA [40].

3.8. Swelling behavior of SR/NR IPNs

The swelling behavior of SR/NR IPNs was evaluated to determine the ability of solvent resistance of SR/NR IPNs. The effects of NR content on swelling behavior of SR/NR IPNs are plotted in Fig. 13. The results showed a significant reduction of swelling ratio of the SR/NR IPNs compared to the SR/NR blends, while the gel content of all SR/NR IPNs was more than 95% indicating that the SR and NR in the curing process were nearly completely incorporated into the polymer networks [41]. It indicated that the formation of IPN can reduce the interaction between polymer and solvent [38] illustrating the enhancement of solvent resistance. The gel fraction corresponded to an increased crosslinking density and the molecular weight between crosslinks of SR/NR IPN obviously decreased.

3.9. Chemical structure of SR/NR IPNs

FT-IR spectra of SR/NR IPNs having different SR/NR mass ratio are presented in Fig. 14. With an incorporation of NR in SR/NR IPN, no changes in characteristic peaks of SR were observed. Moreover, it was noticed that a characteristic peak at 1540 cm^{-1} indicating the presence of zinc stearate with higher intensity at higher NR content. This band could correspond to lower crosslinking density of sulfur-cured in NR chain. The intensity of the peak around 2850 cm^{-1} (assigned to symmetric stretching vibration of C–H bond) was higher at lower SR contents. This result revealed the formation of C–H on Si–CH_2–CH_2–Si during the peroxide vulcanized reaction which was corresponded to the crosslinked structure shown in Fig. 15 [42].

3.10. Morphology study of SR/NR IPNs

The morphology of the SR/NR IPNs are shown in Fig. 16(a)-(b). The results revealed the smooth and uniform morphology of the crosslinked

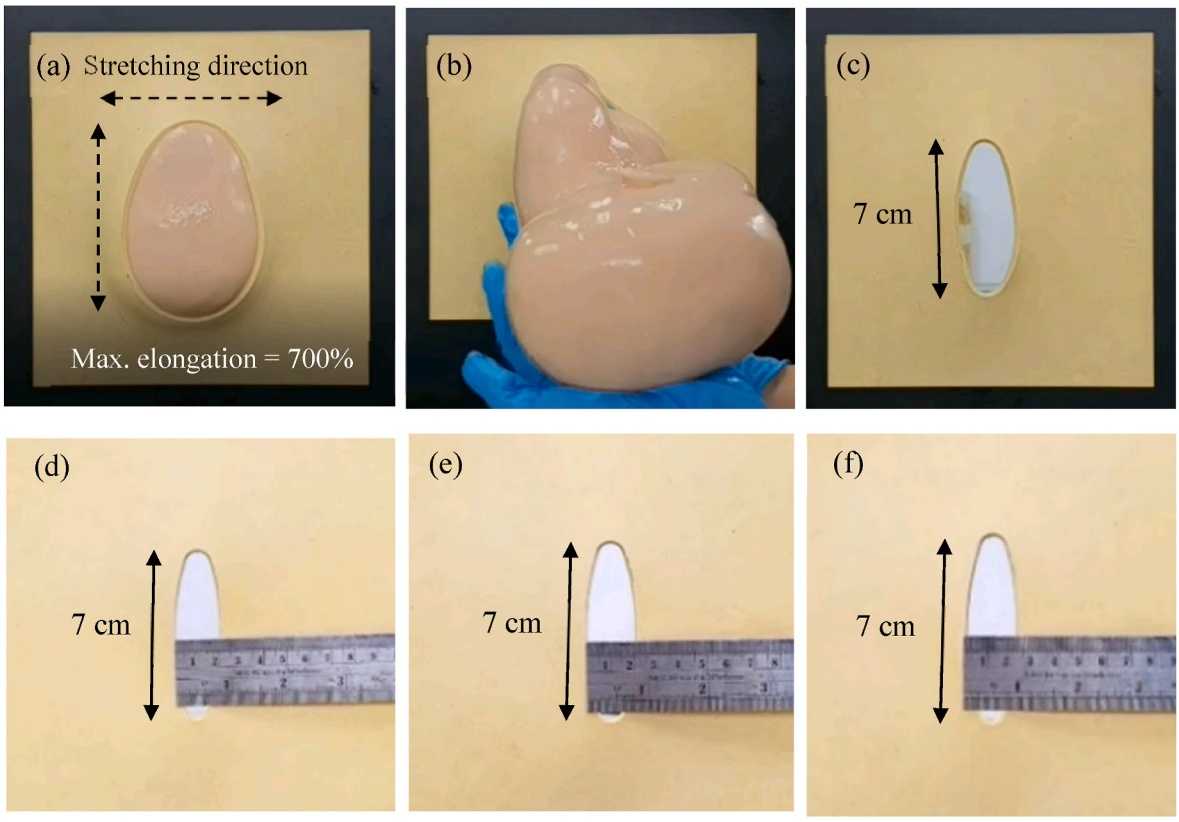

Fig. 18. 2D-birthing model during simulating of childbirth (a)–(c) and childbirth simulation at different fatigue cycles (d) initial or 0^{th}, (e) 1st and (f) 10th cycle.

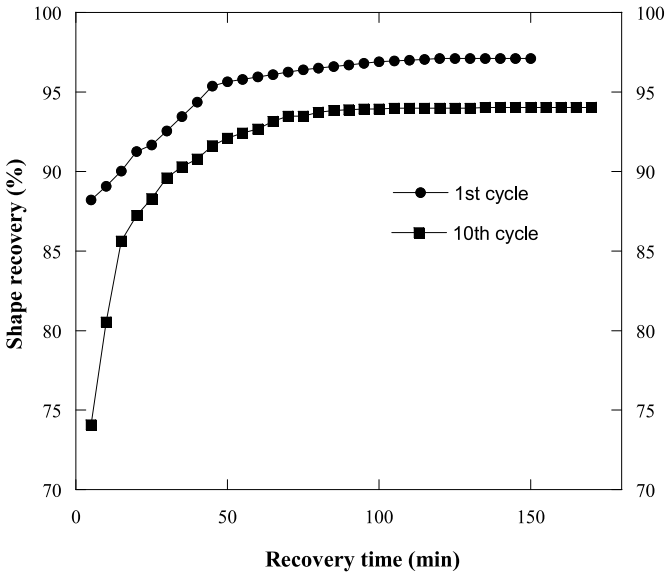

Fig. 19. Shape recovery versus recovery time of simulating childbirth model at stretching ratio of 700% for different fatigue cycles.

SR and NR. The morphology of SR/NR shown in Fig. 16(c)–(e) illustrated the light phase representing continuous SR network where the dark phase (red arrow) is the dispersed phase of interpenetrating network of the phase domains of NR [43]. In comparison, the domain of SR/NR IPN was smaller than that of SR/NR blend resulting in an improvement in load transfer of SR/NR IPN thus enhance mechanical properties [28,44].

3.11. Thermo-mechanical properties of SR/NR polymer hybrid

The prepared polymer networks, as comprised of inorganic and organic components, are characterized as polymer hybrids. The effect of curing system on thermo-mechanical properties of SR/NR polymer hybrids was studied by dynamic mechanical analysis (DMA). The loss tangent and storage modulus curves as a function of temperature are shown in Fig. 17(a) and (b), respectively. The storage modulus at glassy state and glass transition temperature (T_g) obtained from the peak position of loss tangent curve are summarized in Table 3.

From Fig. 17(a), it was observed that the neat SR and NR exhibited single T_g at −110 and −50 °C, respectively. The SR/NR blend showed two $T_{g,s}$ indicating the phase separation of those two rubbers. Moreover, it was observed that the first T_g of SR and NR shifted to lower temperatures. This shows that the network formation of the neat SR by peroxide curing agent gave a higher degree of crosslinking, which restricted the mobility of chain segments leading to the higher T_g of SR than that of the blend. Whereas, the lower T_g of the NR in the blend system is due to the diffusion of SR phase into NR. This result implied that the SR/NR is a partially miscible blend [45]. A similar behavior was also observed in the SR/NR IPN i.e. the SR/NR IPN showed two separated $T_{g,s}$ which were shifted to lower temperatures than those of the neat SR and NR. The DMA curves also showed a broad peak indicating a micro heterogeneous phase separation.

Storage modulus is an important index of rubber elasticity. It can be seen from Fig. 17(b) that the modulus at the glassy state (−150 °C) of the neat SR was higher than that of the neat NR. The storage modulus of the SR/NR blend was between those of the SR and NR. The decrease of storage modulus of the blend than the neat SR could be explained due to the effect of sulfur/peroxide curing system, which reduced the stiffness of SR/NR blend compared to SR cured with peroxide. Moreover, Fig. 17 illustrated the peak and turning point at −35 °C for all samples containing SR [46]. This was attributed to the occurrence of crystallization

in SR elastomers, where SR/NR blend and IPN crystallized in similar manners as SR around −35 °C.

3.12. Tension set of SR/NR polymer hybrids

The tension set annotates the ability of a material to recover to its original shape after removing the tension force. A material with a low-tension set refers to a material that can recover a lot after being stretched. The material having low recovery ability, it indicates the occurrence of permanent deformation within the material due to stretching. Therefore, the tension set is directly related to the elastic properties of the crosslinked polymer. The tension set can be calculated from equation (2) [47]. The tension set of the SR/NR blends (Table 4) was higher than that of the birthing model's material having the value of 11.3%. Whereas, the value of SR/NR IPN was much lower than that of the birthing model's material, due to the higher crosslinking density and swelling ratio of the IPN than these of the blend [47]. It can be seen from the result that the SR/NR blends has a tension set value close to that of the birthing model.

It can be concluded that the SR/NR blend exhibited the most preferable properties to be used as a birthing model than the SR/NR IPN. Consequently, the 2D-birthing model sample was fabricated using the SR/NR blends at a ratio of 90/10 for further mimicking the childbirth practice and study the recovery ability of the material to the original shape. The changes in dimension for simulation of childbirth and the shape recovery of the SR/NR blend dependency on the cycle of childbirth are shown in Figs. 18 and 19, respectively.

Fig. 18 shows the changes in dimension after 10 times of childbirth cycle. It is seen that the height of the hole remained the same to the original height while only width changed. Fig. 19 shows the shape recovery for 1st cycle of childbirth was approximately 97% and up to 10th cycle was shape recovery value of 94%. In terms of recovery time, it was significantly increased upon the increased cycle of childbirth. The result indicated that the SR/NR blend can be used for birthing model's material up to 10 cycles with relatively low dimensional change.

4. Conclusions

The SR/NR blend 90/10 for the birthing model's material was successfully developed. The results from FT-IR spectroscopy revealed a physical interaction between SR and NR, as no new peaks or peak shifts were observed. DSC thermograms of the SR/NR blend showed that the sulfur-cured reaction occurred at a lower temperature followed by a peroxide-cured reaction. Moreover, the SR/NR blend 90/10 showed the highest tensile strength and elongation at break having the values of 1.9 MPa and 1381%, respectively. The SEM micrograph revealed a relatively uniform morphology of the SR/NR blend at a ratio of 90/10. Interestingly, the SR/NR blend exhibited a hardness value in the range of human skin having the value of 20–30 HA, which was preferable for the birthing model compared to that of the IPN system. Furthermore, the SR/NR blend demonstrated a childbirth cycle up to 10 cycles with relatively low dimensional changes. Finally, this developed SR/NR blend at ratio of 90/10 is a promising potential material to substitute the expensive currently used silicone birthing model.

Author contributions

Phanutchanart Panmanee: Investigation and Writing-Original draft preparation. **Manunya Okhawilai:** Methodology and Writing-Review&Editing: **Phattarin Mora**: Investigation. **Chanchira Jubsilp:** Investigation. **Panagiotis Karagiannidis**: Writing-Review&Editing. **Sarawut Rimdusit**: Supervision and Conceptualization.

Declaration of competing interest

The authors declare that they have no known competing financial interests or personal relationships that could have appeared to influence the work reported in this paper.

Data availability

Data will be made available on request.

Acknowledgements

This research has received funding support from the NSRF via the Program Management Unit for Human Resources & Institutional Development, Research and Innovation [grant number B05F640086]. Additional funding is by Thailand Science Research and Innovation Fund, Chulalongkorn University (BCG66210018) and from National Research Council of Thailand.

References

[1] Y.-L. Zhang, C.-G. Zang, L.-P. Shi, Q.-J. Jiao, H.-W. Pan, Y.-F. She-li, Preparation of boron-containing hybridized silicon rubber by in-situ polymerization of vinylphenyl-functionalized polyborosiloxane and liquid silicone rubber, Polymer 219 (2021), 123541, https://doi.org/10.1016/j.polymer.2021.123541.
[2] X. Yang, Q. Li, Z. Li, X. Xu, H. Liu, S. Shang, et al., Preparation and characterization of room-temperature-vulcanized silicone rubber using acrylpimaric acid-modified aminopropyltriethoxysilane as a cross-linking agent, ACS Sustain. Chem. Eng. 7 (2019) 4964–4974, https://doi.org/10.1021/acssuschemeng.8b05597.
[3] J.J. Park, J.Y. Lee, Y.G. Hong, Effects of vinylsilane-modified nanosilica particles on electrical and mechanical properties of silicone rubber nanocomposites, Polymer 197 (2020), 122493, https://doi.org/10.1016/j.polymer.2020.122493.
[4] S. Rimdusit, S. Ratchukul, K. Kamonchaivanich, C. Sopajaree, Breast Model, Thailand Patent no. 63011.
[5] W. Prasomsin, R.B. Prastowo, M. Okhawilai, C. Jubsilp, S. Rimdusit, Development of suture pad from silk fiber reinforced polydimethylsiloxane composite for medical practice, Eng. J. 25 (2021) 71–79, https://doi.org/10.4186/ej.2021.25.5.71.
[6] S.L. Steffensen, M.H. Vestergaard, E.H. Møller, M. Groenning, M. Alm, H. Franzyk, et al., Soft hydrogels interpenetrating silicone–A polymer network for drug-releasing medical devices, J. Biomed. Mater. Res. B Appl. Biomater. 104 (2016) 402–410, https://doi.org/10.1002/jbm.b.33371.
[7] D.W. Schubert, M. Lämmlein, H. von Hanstein, Cyclic loading of model silicone elastomer samples with regard to the failure of silicone breast implants, Polym. Test. 66 (2018) 292–295, https://doi.org/10.1016/j.polymertesting.2018.01.029.
[8] J. Fan, Y. Chen, Z. Jing, M.S. Ibrahim, M. Cai, A Gamma process-based degradation testing of silicone encapsulant used in LED packaging, Polym. Test. 96 (2021), 107090, https://doi.org/10.1016/j.polymertesting.2021.107090.
[9] A. Bannych, S. Katz, Z. Barkay, N. Lachman, Preserving softness and elastic recovery in silicone-based stretchable electrodes using carbon nanotubes, Polymers 12 (2020) 1345, https://doi.org/10.3390/polym12061345.
[10] Z. Li, Y. Shan, X. Wang, H. Li, K. Yang, Y. Cui, Self-healing flexible sensor based on metal-ligand coordination, Chem. Eng. J. 394 (2020), 124932, https://doi.org/10.1016/j.cej.2020.124932.
[11] M. Qi, X. Jia, G. Wang, Z. Xu, Y. Zhang, Q. He, Research on high temperature friction properties of PTFE/Fluorosilicone rubber/silicone rubber, Polym. Test. 91 (2020), 106817, https://doi.org/10.1016/j.polymertesting.2020.106817.
[12] P.S. Sarath, S.V. Samson, R. Reghunath, M.K. Pandey, J.T. Haponiuk, S. Thomas, S. George, Fabrication of exfoliated graphite reinforced silicone rubber composites Mechanical, tribological and dielectric properties, Polym. Test. 89 (2020), 106601, https://doi.org/10.1016/j.polymertesting.2020.106601.
[13] H. Chai, X. Tang, M. Ni, F. Chen, Y. Zhang, D. Chen, Y. Qiu, Preparation and properties of flexible flame-retardant neutron shielding material based on methyl vinyl silicone rubber, J. Nucl. Mater. 464 (2015) 210–215, https://doi.org/10.1016/j.jnucmat.2015.04.048.
[14] J. Lin, H. Zhang, P. Li, X. Yin, Y. Chen, G. Zeng, Electromagnetic shielding of multiwalled, bamboo-like carbon nanotube/methyl vinyl silicone composite prepared by liquid blending, Compos. Interfac. 21 (6) (2014) 553–569, https://doi.org/10.1080/15685543.2014.899191.
[15] J. Xu, Y. Zhang, Y.B. Feng, T. Qiu, G. Wang, R. Liu, Electromagnetic and mechanical properties of carbonyl iron powder-filled methyl vinyl silicone rubber during thermal aging, Polym. Compos. 39 (2018) 2897–2903, https://doi.org/10.1002/pc.24286.
[16] T. Dang, J. Kim, S. Hoon Lee, K. Jea, Kim Vinyl functional group effects on mechanical and thermal properties of silica-filled silicone rubber/natural rubber blends, Compos. Interfac. 18 (2011) 151–168, https://doi.org/10.1163/092764411X567558.
[17] T.T.N. Dang, J.K. Kim, K.J. Kim, Organo bifunctional silane effects on the vibration, thermal, and mechanical properties of a vinyl-group-containing silicone rubber/natural rubber/silica compound, J. Vinyl Addit. Technol. 16 (2010) 254–260, https://doi.org/10.1002/vnl.20240.
[18] H. Magaña, C.D. Becerra, A. Serrano-Medina, K. Palomino, G. Palomino-Vizcaíno, A. Olivas-Sarabia, et al., Radiation grafting of a polymeric prodrug onto silicone

rubber for potential medical/surgical procedures, Polymers 12 (2020) 1297, https://doi.org/10.3390/polym12061297.
[19] K. Matsuura, H. Saito, Tensile properties, and interfacial adhesion of silicone rubber/polyethylene blends by reactive blending, J. Appl. Polym. Sci. 135 (2018), 46192, https://doi.org/10.1002/app.46192.
[20] P. Jaroenthonkajonchai, Effect of sulfenamide accelerators, chemical blowing agent and graphene on formation and properties of natural rubber foam, in: Chemical Engineering, Chulalongkorn University, 2015.
[21] J. Kruzelak, A. Kvansicakova, R. Dosoudil, I. Hudec, J. Vilcakova, Combined sulfur and peroxide curing systems applied in cross-linking of rubber magnets, Polym. Polym. Compos. 29 (2021) 1155–1166, https://doi.org/10.1177/0967391120956508.
[22] J. Kruzelak, R. Dosoudil, R. Sykora, I. Hudec, Rubber composites cured with sulphur and peroxide and incorporated with strontium ferrite, Bull. Mater. Sci. 40 (2017) 223–231, https://doi.org/10.1007/s12034-016-1347-z.
[23] D. Ma, L. Wu, S. Feng, H. Lu, S. Zhao, Effect of yttrium phosphate on irradiation of methyl vinyl silicone rubber, Radiat. Phys. Chem. 136 (2017) 44–49, https://doi.org/10.1016/j.radphyschem.2017.03.024.
[24] J. Martin, Kinetic analysis of two DSC peaks in the curing of an unsaturated polyester resin catalyzed with methylethylketone peroxide and cobalt octoate, Polym. Eng. Sci. 47 (2007) 62–70, https://doi.org/10.1002/pen.20667.
[25] A. Wattanakornsiri, T. Jamnongkan, Influence of crosslinking agent on the kinetics and mechanisms of swelling behavior of poly(vinyl alcohol) hydrogel), in: The 39th National Graduate Research Conference, 2016, pp. 367–375.
[26] N. Rimdusit, C. Jubsilp, P. Mora, K. Hemvichian, T.T. Thuy, P. Karagiannidis, S. Rimdusit, Radiation graft-copolymerization of ultrafine fully vulcanized powdered natural rubber: effects of styrene and acrylonitrile contents on thermal stability, Polymers 13 (2021) 3447, https://doi.org/10.3390/polym13193447.
[27] D. Thomas, Stress/strain and swelling properties of a peroxide-cured methylvinyl silicone, Polymer 6 (1964) 463–470, https://doi.org/10.1016/0032-3861(64)90194-6.
[28] Q. Wang, S. Chen, T. Wang, in: S. Thomas, D. Grande, U. Cvelbar, K.V.S.N. Raju, R. Narayan, S.P. Thomas, H. Akhina (Eds.), Synthetic Rubber-Based IPNs. Micro- and Nano-Structured Interpenetrating Polymer Networks: from Design to Applications, John Wiley & Sons, Inc, 2016, pp. 69–107, https://doi.org/10.1002/9781119138945.ch3.
[29] G. Gallo, E. Erdmann, C.N. Cavasotto, Evaluation of silicone fluids and resins as CO2 thickeners for enhanced oil recovery using a computational and experimental approach, ACS Omega 6 (2021) 24803–24813, https://doi.org/10.1021/acsomega.1c03660.
[30] .
[31] W. Fang, X. Fan, R. Li, Preparation of polyoxymethylene/methyl vinyl silicone rubber/thermoplastic polyurethane ternary thermoplastic vulcanizates with good toughness properties, J. Thermoplast. Compos. Mater. (2021) 1–14, https://doi.org/10.1177/08927057211057113, 0.
[32] L. Kruželák, A. Kvasničáková, R. Dosoudil, Thermo-oxidative stability of rubber magnetic composites cured with sulfur, peroxide and mixed curing systems, Plast., Rubber Compos. 47 (2018) 324–336, https://doi.org/10.1080/14658011.2018.1492270.
[33] O. Boondamnoen, A.R. Azura, M. Ohshima, S. Chuayjuljit, Effect of blend ratio and compatibilizer on solution casted treated waste natural rubber latex/polystyrene blends, Songklanakarin J. Sci. Technol. 35 (2013) 547–555.
[34] B. Kuriakose, S.K. Chakraborty, S.K. De, Scanning electron microscopy studies on tensile failure of thermoplastic elastomers from polypropylene-natural rubber blends, Mater. Chem. Phys. 12 (1985) 157–170, https://doi.org/10.1016/0254-0584(85)90053-7.
[35] B. Narupai, M. Leekrajang, N. Chutichairattanaphum, S. Larpkiattaworn, J. Panichpakdee, P. Somwongsa, The effects of silica/carbon black hybrid filler contents on natural rubber composite properties using conventional vulcanization system, Int. J. Innov. Sci. Technol. 3 (2020) 13–23.
[36] I.M. Meththananda, S. Parker, M.P. Patel, M. Braden, The relationship between Shore hardness of elastomeric dental materials and Young's modulus, Dent. Mater. J. 25 (2009) 956–959, https://doi.org/10.1016/j.dental.2009.02.001.
[37] C. Roland, Interpenetrating Polymer Networks (IPN Q1): Structure and Mechanical Behavior, Encyclopedia of polymeric nanomaterials, 2013, pp. 1–9.
[38] J. Johns, C. Nakason, Novel interpenetrating polymer networks based on natural rubber/poly (vinyl alcohol), Polym. Plast. Technol. Eng. 51 (2012) 1046–1053, https://doi.org/10.1080/03602559.2012.689053.
[39] Ł. Zedler, X. Colom, J. Cañavate, M. Reza Saeb, J. Haponiuk, K. Formela, Investigating the impact of curing system on structure-property relationship of natural rubber modified with brewery by-product and ground tire rubber, Polymers 12 (2020) 545, https://doi.org/10.3390/polym12030545.
[40] S. Panduri, V. Dini, M. Romanelli, The Durometer Measurement of the Skin: Hardware and Measuring Principles. Agache's Measuring the Skin, Springer, Cham, 2017.
[41] Z. Wang, P. Gnanasekar, S.S. Nair, S. Yi, N. Yan, Curing behavior and thermomechanical performance of bioepoxy resin synthesized from vanillyl alcohol: effects of the curing agent, Polymers 13 (2021) 2891, https://doi.org/10.3390/polym13172891.
[42] J. Ji, X. Ge, X. Pang, R. Liu, S. Wen, J. Sun, W. Liang, J. Ge, X. Chen, Synthesis and characterization of room temperature vulcanized silicone rubber using methoxyl-capped MQ silicone resin as self-reinforced cross-linker, Polymers 11 (2019) 1142, https://doi.org/10.3390/polym11071142.
[43] V.J. Dave, H.S. Patel, Synthesis and characterization of interpenetrating polymer networks from transesterified castor oil based polyurethane and polystyrene, J. Saudi Chem. Soc. 21 (2017) 18–24, https://doi.org/10.1016/j.jscs.2013.08.001.
[44] M. Liu, G. Song, J. Yi, Y. Xu, Damping analysis of polyurethane/polyacrylate interpenetrating polymer network composites filled with graphite particles, Polym. Compos. 34 (2013) 288–292, https://doi.org/10.1002/pc.22395.
[45] W. Wu, Y. Wang, Vulcanization and thermal properties of silicone rubber/fluorine rubber blends, J. Macromol. Sci. B. 58 (2019) 579–591, https://doi.org/10.1080/00222348.2019.1609214.
[46] Y. Huang, Q. Mu, Z. Su, High and low temperature resistance of phenyl silicone rubber, in: IOP Conference Series: Materials Science and Engineering, IOP Publishing, 2021, https://doi.org/10.1088/1757-899X/1048/1/012001.
[47] N. Kunanusont, C. Samthong, F. Bowen, M. Yamaguchi, A. Somwangthanaroj, Effect of mixing method on properties of ethylene vinyl acetate copolymer/natural rubber thermoplastic vulcanizates, Polymers 12 (2020) 1739, https://doi.org/10.3390/polym12081739.